

The respiratory chain inhibitor rotenone affects peroxisomal dynamics via its microtubule-destabilizing activity

Josiah B. Passmore^{1#}, Sonia Pinho^{2#}, Maria Gomez-Lazaro^{2,3}, and Michael
Schrader^{1,2*}

¹College of Life and Environmental Sciences, Biosciences, University of Exeter,
Exeter, UK

²Center for Cell Biology & Dept. of Biology, University of Aveiro, Aveiro,
Portugal

³Instituto de Investigação e Inovação em Saúde (i3S) & Instituto de Engenharia
Biomédica (INEB), University of Porto, Porto, Portugal

equal first author contribution

* Address all correspondence to Michael Schrader, College of Life and Environmental
Sciences, Biosciences, University of Exeter, Geoffrey Pope Building, Stocker Road, Exeter
EX4 4QD, UK

E-mail: m.schrader@exeter.ac.uk

ORCID IDs orcid.org/: J.P. 0000-0001-7791-3439; S.P. 0000-0002-7426-5197; M.G.L.0000-
0002-8836-396X; M.S. 0000-0003-2146-0535

Character count:20365

Abstract

Peroxisomes and mitochondria in mammalian cells are closely linked subcellular organelles, which maintain a redox-sensitive relationship. Their interplay and role in ROS signalling is supposed to impact on age-related and degenerative disorders. Whereas the generation of peroxisome-derived oxidative stress can affect mitochondrial morphology and function, little is known about the impact of mitochondria-derived oxidative stress on peroxisomes. Here, we investigated the effect of the mitochondrial complex I inhibitor rotenone on peroxisomal and mitochondrial membrane dynamics. We show that rotenone treatment of COS-7 cells alters peroxisome morphology and distribution. However, this effect is related to its microtubule-destabilising activity rather than to the generation of oxidative stress. Rotenone also induced alterations in mitochondrial morphology, which – in contrast to its effect on peroxisomes - were dependent on the generation of ROS but independent of its microtubule-active properties. The importance of our findings for the peroxisome-mitochondria redox relationship and the interpretation of *in cellulo* and *in vivo* studies with rotenone, which is widely used to study Parkinson's disease, are discussed.

Keywords: peroxisomes, mitochondria, rotenone, ROS, organelle cooperation

Abbreviations: NAC, N-acetyl cysteine ; ROS, reactive oxygen species ; ROT, rotenone ; TAX, paclitaxel ;

Introduction

Peroxisomes are ubiquitous and dynamic single membrane-bound organelles in eukaryotic cells, that - similar to mitochondria - show an oxidative type of metabolism. Peroxisomes perform important functions in hydrogen peroxide and lipid metabolism rendering them essential for human health and development (Wanders and Waterham 2006). To fulfil their multiple functions, peroxisomes need to communicate and cooperate with other organelles, including mitochondria, the endoplasmic reticulum (ER) or lipid droplets (Schrader et al. 2013; Schrader et al. 2015a; 2015b; Gao and Goodman 2015; Costello et al. 2017). Over the years, substantial evidence has been provided for a close functional interplay between peroxisomes and mitochondria (the so-called “peroxisome-mitochondria connection”) which impacts on human health and development (Schrader and Yoon 2007; Camoes et al. 2009; Schrader et al. 2015a). Peroxisomes and mitochondria in mammalian cells cooperate metabolically in the breakdown of fatty acids by β -oxidation (reviewed in Wanders et al. 2016), they maintain a redox-sensitive relationship (reviewed in Lismont et al. 2015), share key components of the membrane fission machineries (reviewed in Schrader et al. 2012, 2016), cooperate in anti-viral signalling (Dixit et al. 2010; Odendall et al. 2014) and may depend on each other for biogenesis and functionality (Peeters et al. 2011, 2015; Mohanty and McBride 2013; Sugiura et al. 2017). Of particular interest are their redox-sensitive relationship and their interplay and communication with respect to ROS signalling, which may impact on age-related and degenerative disorders (Koepke et al. 2008; Ivashchenko et al. 2011; Walton and Pizzitelli, 2012; Titorenko and Terlecky 2011; Beach et al. 2012; Fransen et al. 2013; Nordgren and Fransen 2014). The generation of oxidative stress in peroxisomes has been shown to impact on mitochondrial morphology and function (Ivashchenko et al. 2011; Wang et al. 2013). However, little is known about the impact of mitochondria-derived oxidative stress on peroxisomes. Here, we have examined the effect of the potent complex I inhibitor rotenone on peroxisomal and mitochondrial membrane dynamics. We show that

although rotenone has an impact on peroxisome morphology and distribution, this effect is related to its microtubule-destabilising activity rather than to oxidative stress. On the other hand, rotenone induced alterations in mitochondrial morphology, which were dependent on the generation of ROS but independent of its microtubule-active properties.

Materials and methods

Antibodies

Antibodies were used as follows: rabbit polyclonal antibody against PEX14 (1:1400, kindly provided by D. Crane, Griffith University, Brisbane, Australia) (Nguyen et al. 2006; Grant et al. 2013), mouse monoclonal antibodies against α -tubulin (Sigma, T9026) and acetylated α -tubulin (Sigma, T6793) (both used at 1:200 for immunofluorescence, 1:1000 for immunoblotting), and TOM20 (1:200 for immunofluorescence) (BD Transduction Laboratories, San Diego, USA; 612278). Secondary anti-IgG antibodies against rabbit (Alexa 488, 1:500; A21206) and mouse (Alexa 488, 1:400, A21202 and Alexa 594, 1:1000, A21203) were obtained from Molecular Probes (as part of Invitrogen Life Technologies, Eugene, USA). Anti-mouse IgG antibodies conjugated to HRP (1:5000, 170-6516) were obtained from Bio-Rad (Munich, Germany). The specificity of all antibodies has been validated in several previous studies.

Cell culture and drug treatment

COS-7 (African green monkey kidney cells; ATCC CRL-1651) were cultured in DMEM, high glucose (4.5 g/L) supplemented with 10% FBS, penicillin and streptomycin (all from Life Technologies) at 37°C with 5% CO₂ and 95% humidity (HERACell 240i CO₂ incubator). Cells were seeded onto glass coverslips (Fisher Scientific, 19 mm Ø, 0.13-0.17 mm thickness) at a defined density (1×10^5 cells/ml). 24 hours after seeding, the culture medium was aspirated, and cells were treated for different time intervals (3, 6 and 24 hours) with a range of concentrations of rotenone (Sigma, R8875) (100 nM, 1 μ M, 10 μ M, 100 μ M, 1 mM). For pre-treatment with the microtubule-stabilizing drug paclitaxel (taxol) (Sigma, T7402), cells were first incubated with 20 μ M paclitaxel for 6 hours before the addition of rotenone. For pre-treatment with the antioxidant N-acetyl cysteine (NAC) (Sigma, A7250), cells were first incubated with 10 mM NAC for 1 hour before the addition of rotenone. Stock concentrations

of 100 mM rotenone and 2 mM paclitaxel were prepared in dimethyl sulfoxide (DMSO) (Sigma, D8418) and dilutions prepared in culture medium. A stock concentration of 100 mM NAC was prepared always fresh in culture medium, and diluted in culture medium following pH neutralization and sterilization by filtration of the stock.

Immunofluorescence and microscopy

Cells grown on glass coverslips were washed twice with phosphate-buffered saline (PBS). Cells to be stained with organelle markers (e.g. PEX14 or TOM20) were fixed using 4% paraformaldehyde, pH 7.4 for 20 minutes at room temperature as previously described (Bonekamp et al. 2013) as peroxisome morphology is sensitive to alcoholic fixation (Schrader et al. 1995). Cells to be stained with cytoskeletal markers (e.g. α -tubulin or acetylated α -tubulin) were fixed with ice-cold methanol for 15 minutes at -20°C . Following fixation cells were washed 3 times in PBS, membranes were permeabilised with 0.2% Triton X-100 for 10 minutes at room temperature (permeabilisation was omitted for methanol-fixed cells), washed again 3 times in PBS and blocked with 2% bovine serum albumin (BSA) for 10 minutes at room temperature. Cells were then incubated for 1 hour with primary antibodies diluted in PBS, washed 3 times in PBS and incubated for 1 hour with secondary antibodies diluted in PBS. In controls, where the primary antibodies were omitted, no staining reactions were observed. To mount coverslips on slides, cells were washed 3 times in PBS, dipped in dH_2O and mounted (after removal of excess water) in Mowiol 4-88 containing n-propyl galate as an anti-fading (Bonekamp et al. 2013). Cell imaging was performed using an Olympus IX81 microscope with an UPlanSApo 100x/1.40 Oil objective (Olympus Optical, Hamburg, Germany), eGFP ET filter-set (470/40 Et Bandpass filter, Beamsplitter T495 LPXR and 525/50 ET Bandpass filter (Chroma Technology GmbH, Olching, Germany)), TxRed HC Filter Set (562/40 BrightLine HC Beamsplitter HC BS 593, 624/40 BrightLine HC (Semrock, Rochester, USA)). Images were taken with a CoolSNAP HQ2 CCD camera (150-300 ms

exposure, gain 3, bin 1, gamma 1) and MetaMorph 7 (Molecular Devices, USA) was used to adjust for contrast and brightness.

Gel electrophoresis and immunoblotting

Following drug treatment, cells were trypsinised, washed in PBS and centrifuged at $500 \times g$ for 3 min. Cell pellets were lysed (25 mM Tris-HCl, pH 8.0, 150 mM NaCl, 0.5% sodium deoxycholate, 1.5mM Triton X-100 and a protease-inhibitor mix (Roche Diagnostics)) and protein concentrations were determined using the Bradford assay (Bradford 1976) (Bio-Rad Protein Assay Dye Reagent Concentrate, 5000006). Equal amounts of protein were separated by SDS-PAGE on 12.5% polyacrylamide gels, transferred to nitrocellulose membrane (Amersham Bioscience, Arlington Heights, IL, USA) using a semi-dry apparatus (Trans-Blot SD, Biorad) and analysed by immunoblotting using the corresponding primary antibodies and horseradish peroxidase-conjugated secondary antibodies and enhanced chemiluminescence reagents (Amersham Bioscience, Arlington Heights, IL, USA).

Measurement and quantification of ROS production

Intracellular ROS levels were measured using the fluorescent dye 2', 7'-dichlorodihydrofluorescein diacetate (H₂DCFDA) (Molecular Probes, Life Technologies). H₂DCFDA is intracellularly oxidized by ROS, producing the fluorescent compound dichlorofluorescein (DCF), which can be detected by measuring the fluorescence at 530 nm when excited at 485 nm (Fernandez-Gomez et al. 2006; Perez-Ortiz et al. 2004). Cells were seeded in 96-well culture plates (10^4 cells/well) (Greiner Bio-One) and treated with rotenone after 24 hours. At different time points, the medium was removed and the cells were washed one time with PBS. Cells were incubated with 10 μ M H₂DCFDA and the fluorescence intensity was measured immediately every 5 minutes over a period of 30 minutes in a

multifunctional microplate reader (TECAN i-control – infinite 200, Austria GmbH). An average of 4 to 6 wells per condition was measured and a mean value obtained. Controls included untreated cells, a blank containing cell culture medium and dye; and H₂O₂ together with the dye as a positive control). A linear increase of fluorescence with time was plotted and used to calculate a linear regression. From this the average relative percentage of ROS production was determined from at least 3 independent experiments.

Quantification and statistical analysis of data

Analysis of statistical significance was performed using GraphPad Prism 5 software. A two-tailed unpaired t-test was used to determine statistical difference against the indicated group. *p<0.05, **p<0.01, ***p<0.001. For analysis of organelle distribution and morphology, a minimum of 150 cells were examined per condition, and organelle parameters (e.g. tubular, elongated morphology, intracellular distribution/clustering) were microscopically assessed in at least 3 independent experiments. The analysis was made blind and in different areas of the coverslip. Data are presented as mean ± SD.

Results and Discussion

Rotenone alters peroxisome morphology and distribution

Rotenone, an agricultural pesticide, is well known to inhibit complex I (NADH CoQ1 reductase) in the mitochondrial respiratory chain (Chance et al. 1963; Higgins and Greenamyre 1996). It is a widely used toxin employed in animal and cellular models of Parkinson's disease and can freely cross cell membranes (Betarbet et al. 2000; Alam et al. 2002; Mounsey and Teismann 2010). Chronic treatments with rotenone in mice reproduce some features of this disease such as motor deficits, protein aggregation, and loss of dopaminergic neurons (Meurers et al. 2009). Complex I inhibition has several potential functional consequences, including ATP depletion, which in turn induces oxidative stress in cells (Sherer et al. 2003; Testa et al. 2005). To examine whether an inhibitor of the mitochondrial respiratory chain known to produce ROS exhibits an effect on the peroxisomal compartment, COS-7 cells were treated with different concentrations of rotenone (100 nM, 1 μ M, 10 μ M, 100 μ M, 1 mM). Treated cells and controls were processed for immunofluorescence after 6 and 24 hours, and peroxisomes were labelled with antibodies against Pex14, a peroxisomal membrane protein (Fig. 1). Peroxisomes in COS-7 cells are uniformly distributed in the cytoplasm, and are usually spherical in shape (Fig. 1a) (Koch et al. 2004; Lin et al. 2016). Treatment with rotenone induced a concentration-dependent elongation of the peroxisomal compartment (Fig. 1b, e) as well as clustering of peroxisomes (Fig. 1c, f) and an uneven distribution of the organelles in the cytoplasm (Fig. 1d). Cells showed either tubular or clustered peroxisomes or a mixture of both. Peroxisome elongation is a pre-requisite of peroxisome multiplication by growth and division (Schrader et al. 2012; 2016), and tubular peroxisomes can be induced by different stimuli including growth factors, fatty acids, and ROS (Schrader et al. 1998; 1999; Schrader and Fahimi 2006). However, peroxisome elongation, clustering and altered distribution has also been observed under conditions of microtubule-depolymerisation (Schrader et al. 1996; Wiemer et al. 1997), as

peroxisome motility and distribution depends on microtubules in mammalian cells (Schrader et al. 1996; 2003; Wiemer et al. 1997; Lin et al. 2016). Furthermore, rotenone has been reported to inhibit microtubule polymerization and to arrest cell cycle progression at mitosis (Meisner and Sorensen 1966; Brinkley et al. 1974; Marshall and Himes 1978; Srivastava and Panda 2007). We thus investigated microtubule integrity after treatment of COS-7 cells with rotenone.

Rotenone exerts a microtubule-destabilising activity in COS-7 cells

COS-7 cells were treated with different concentrations of rotenone and methanol-fixed. Controls and treated cells were stained with antibodies to α -tubulin (Fig. 2). In controls, microtubules form the typical radial arrays originating from the microtubule-organising centre (MTOC) in interphase cells (Fig. 2a). At low rotenone concentrations, microtubules were still visible and appeared unaffected (Fig. 2b, c). At an intermediate concentration of 10 μ M, some microtubules remained, but the majority was depolymerised (Fig. 2d). Treatment with higher rotenone concentrations resulted in a complete depolymerisation of microtubules (Fig. 2e, f). The effect of rotenone on microtubules was similar after 3, 6 and 24 hours.

To investigate microtubule integrity at low rotenone concentrations, microtubules were stained with an antibody to acetylated α -tubulin (Fig. 2g-i, j). Acetylated α -tubulin is present in various microtubule structures and plays a role in the stabilization of microtubules (Piperno et al. 1987). In control cells only a few microtubules were labelled per cell (Fig. 2g). Interestingly, cells treated with low concentrations of rotenone showed a prominent increase in microtubules containing acetylated α -tubulin (Fig. 2h, i). An increase in acetylated tubulin was confirmed by immunoblotting of cell lysates from controls and rotenone-treated cells (Fig. 2j). These findings indicate that although microtubules appear unaffected in cells treated with low concentrations of rotenone based on α -tubulin staining, they already display posttranslational modifications such as acetylation. Tubulin acetylation likely serves to

stabilise microtubules and to counteract the destabilising activity of rotenone. It has been suggested that rotenone inhibits microtubule assembly by binding to tubulin thus inducing a conformational change in tubulin (Srivastava and Panda 2007).

Alterations in peroxisome distribution induced by rotenone are caused by microtubule depolymerisation

To investigate if peroxisome alterations induced by rotenone are primarily caused by microtubule depolymerisation (or alternatively by Complex I inhibition and oxidative stress), we first pre-incubated COS-7 cells with the microtubule-stabilising agent paclitaxel prior to the addition of rotenone (Fig. 3). Paclitaxel, which causes the formation of microtubule bundles (Fig. 3a, b) protected the microtubules against the microtubule-depolymerising activity of rotenone, even when high concentrations of rotenone were applied (Fig. 3c, d). Interestingly, addition of rotenone after the stabilization of microtubules with paclitaxel showed no effect on peroxisomes (Fig. 3g-i). Peroxisome distribution was mostly uniform, and clustering was similar to the paclitaxel-treated control (Fig. 3g-i). It should be noted that paclitaxel alone increased cluster formation in COS-7 cells when compared to untreated controls, but this was mainly due to fragmentation of the nucleus, which affected the uniform distribution of peroxisomes in the cytoplasm (Fig. 3b, f). As peroxisome elongation is influenced by many factors (e.g. culture condition, cell density) (Schrader et al. 1996; Schrader and Fahimi 2006), we focussed on the analysis of peroxisomal distribution. However, rotenone-induced peroxisome elongation was no longer observed after pre-treatment with paclitaxel (Fig. 3g, h) and not different from controls (Fig. 3e, f) (unpublished observation). Our findings are in line with previous findings showing that paclitaxel provides protective effects against rotenone-induced toxicity (Jiang et al. 2006). Moreover, paclitaxel had no effect on the morphology and distribution of peroxisomes in HepG2 cells, but pre-treatment with paclitaxel and stabilization of microtubules prevented alterations of

peroxisome morphology and distribution caused by microtubule-depolymerising agents such as nocodazole (Schrader et al. 1996). The results show that the effect of rotenone on peroxisomes in mammalian cells is similar to the action of the microtubule-depolymerising drugs nocodazole, colcemid and vinblastine (Schrader et al. 1996). We suggest that peroxisome alterations in mammalian cells induced by rotenone are mainly caused by the microtubule-destabilising activity of rotenone rather than via complex I inhibition and oxidative stress.

Rotenone-induced intracellular ROS are not the major cause of peroxisome alterations in COS-7 cells

Rotenone interferes with the mitochondrial electron transport chain, by inhibiting the transfer of electrons from iron-sulphur centres in complex I to ubiquinone. This prevents NADH from being converted into usable cellular energy (ATP) and consequently leads to ROS production. To examine if peroxisome alterations are a consequence of rotenone-dependent ROS production, intracellular ROS levels were measured in COS-7 cells under control conditions and after treatment with 100 nM rotenone (a concentration not affecting microtubule integrity) using 2',7'-dichlorodihydrofluorescein diacetate (H₂DCFDA) which is intracellularly oxidized by ROS, producing the fluorescent compound dichlorofluorescein (DCF). As shown in Fig. 4a, rotenone increases intracellular ROS levels in COS-7 cells after 6 hours ($276 \pm 6\%$) and 24 hours ($414 \pm 18\%$) when compared to control conditions. Furthermore, pre-treatment of COS-7 cells with the antioxidant N-acetyl cysteine (NAC) prior to the addition of rotenone reduced intracellular ROS levels (Fig. 4a). These findings are in line with published results (Bonet-Ponce et al. 2016). More importantly, pre-treatment with NAC prior to the addition of rotenone did not prevent clustering of peroxisomes and changes in the uniform distribution of the organelle (Fig. 4b). NAC alone only induced a slight increase in peroxisomal clusters compared to control conditions. These observations support our

assumption that peroxisome alterations in mammalian cells induced by rotenone are mainly caused by the microtubule-destabilising activity of rotenone and not via complex I inhibition and increased intracellular ROS levels.

Rotenone alters mitochondrial morphology in a ROS dependent manner

Next, we investigated the morphology of mitochondria in COS-7 cells treated with different concentrations of rotenone. Treated cells and controls were processed for immunofluorescence, and mitochondria were labelled with antibodies against TOM20, a mitochondrial outer membrane protein (Fig. 5). Mitochondria in COS-7 cells usually display an elongated, tubular and bulbous morphology (Fig. 5a, e, i) (Koch et al. 2004). In contrast to its elongating effect on peroxisomes (Fig. 1), rotenone induced a concentration- and time-dependent fragmentation of mitochondria resulting in a spherical, round organelle phenotype (Fig. 5b, c, d). Pre-treatment of COS-7 cells with paclitaxel to stabilise microtubules did not prevent mitochondrial fragmentation (Fig. 5e-h). However, pre-treatment of COS-7 cells with the antioxidant NAC prevented mitochondrial fragmentation even at high rotenone concentrations and maintained a tubular mitochondrial morphology (Fig. 5i-l). These findings indicate that mitochondrial alterations in mammalian cells induced by rotenone are mainly caused by complex I inhibition and increased intracellular ROS levels rather than via the microtubule-destabilising activity of rotenone, which is in contrast to its action on peroxisomes.

We conclude from these observations that at low concentrations (100 nM -10 μ M) rotenone acts on mitochondria in COS-7 cells and induces their fragmentation, likely due to inhibition of complex I and subsequent oxidative stress/increased intracellular ROS levels. Microtubules at these concentrations are still intact (Fig. 2), although exhibiting increased levels of acetylated α -tubulin (Fig. 2). Alterations in peroxisome morphology and distribution are more

prominent at higher rotenone concentrations, as they are induced by the microtubule-depolymerising activity of rotenone, and not primarily via increased intracellular ROS levels. Our findings support published data indicating that mitochondria are more susceptible to changes in cellular redox homeostasis and increased ROS levels than peroxisomes. For example, the neurotoxin 6-Hydroxydopamine, which is supposed to cause ROS generation (Galindo et al. 2003), induced a profound mitochondrial fragmentation in SH-SY5Y neuroblastoma cells, but failed to induce any changes in peroxisome morphology (Gomez-Lazaro et al. 2008). In line with this, we observed no effect on peroxisome morphology when other inhibitors of mitochondrial respiration were used (e.g. sodium azide, an inhibitor of cytochrome c oxidase/complex IV) (unpublished observations). Furthermore, peroxisomes were found to resist oxidative stress generated elsewhere in the cell, whereas generation of excess ROS inside peroxisomes perturbed the mitochondrial redox balance and led to mitochondrial fragmentation and cell death (Ivashchenko et al. 2011; Wang et al. 2013). How redox communication between peroxisomes and mitochondria is mediated, is currently unclear, but may involve a more complex signalling system as opposed to simple diffusion of excess ROS (Lismont et al. 2015).

Our data also indicate that *in cellulo* and *in vivo* studies with rotenone, which has been widely used to study Parkinson's disease (Betarbet et al. 2000), have to be carefully interpreted due to the different effects of rotenone in mammalian cells. We show that besides increasing intracellular ROS levels, mitochondrial fragmentation, and microtubule depolymerisation, rotenone also has an effect on peroxisome dynamics and distribution. Such processes are important for the formation of peroxisomes by growth and division, their intracellular positioning, movement and interaction with other subcellular compartments and have been linked to human health and disease (Schrader et al. 2015a; Ribeiro et al. 2012). Mitochondrial dysfunction is commonly accepted as having a key role in Parkinson's disease, however, microtubule alterations are also considered. For example, 1-methyl-4-phenyl-1,2,3,6-

tetrahydropyridine (MPTP), another model toxin for Parkinson's disease, impacts on microtubule polymerization besides its effect on mitochondria (Cartelli et al. 2010). Disrupting the microtubule network can alter vesicular and organelle transport in neurons leading to neuronal death (Ren et al. 2005; De Vos et al. 2008; Cartelli et al. 2010). Loss of peroxisome dynamics and distribution may contribute to this process.

Acknowledgements

We would like to acknowledge the support of T. A. Schrader, N. A. Bonekamp and J. Jordan (University of Castilla-La Mancha, Albacete, Spain). This work was supported by the Biotechnology and Biological Sciences Research Council (BB/K006231/1, BB/N01541X/1 to M.S.), the Portuguese Foundation for Science and Technology and FEDER/COMPETE (SFRH/BPD/37725/2007 to M.G.L), the University of Aveiro, PT and CLES, University of Exeter, UK. M.S. is supported by a Marie Curie Initial Training Network (ITN) action PerFuMe (316723).

Conflict of interest

The authors do not declare a conflict of interest.

References

- Alam M, Schmidt WJ (2002) Rotenone destroys dopaminergic neurons and induces parkinsonian symptoms in rats. *Behav Brain Res* 136(1):317-324
- Beach A, Burstein MT, Richard VR, Leonov A, Levy S, Titorenko VI (2012) Integration of peroxisomes into an endomembrane system that governs cellular aging. *Front Physiol* 3:283
- Betarbet R, Sherer TB, MacKenzie G, Garcia-Osuna M, Panov AV, Greenamyre JT (2000) Chronic systemic pesticide exposure reproduces features of Parkinson's disease. *Nat Neurosci* 3:1301–1306
- Bonekamp N, Islinger M, Gomez-Lazaro M, Schrader M (2013) Cytochemical detection of peroxisomes and mitochondria. *Methods Mol Biol* 931:467-82
- Bonet-Ponce L, Saez-Atienzar S, da Casa C, Sancho-Pelluz J, Barcia JM, Martinez-Gil N, Nava E, Jordan J, Romero FJ, Galindo MF (2016) Rotenone Induces the Formation of 4-Hydroxynonenal Aggregates. Role of ROS-Mediated Tubulin Hyperacetylation and Autophagic Flux Disruption. *Mol Neurobiol* 53(9):6194-6208
- Bradford MM (1976) A rapid and sensitive method for the quantitation of microgram quantities of protein utilizing the principle of protein-dye binding. *Anal Biochem* 72:248-254
- Brinkley BR, Barham SS, Barranco SC, Fuller GM (1974) Rotenone inhibition of spindle microtubule assembly in mammalian cells. *Exp Cell Res* 85:41–46
- Camões F, Bonekamp NA, Delille HK, Schrader M (2009) Organelle dynamics and dysfunction: A closer link between peroxisomes and mitochondria. *J Inher Metab Dis* 32(2):163-180
- Cartelli D, Ronchi C, Maggioni MG, Rodighiero S, Giavini E, Cappelletti G (2010) Microtubule dysfunction precedes transport impairment and mitochondria damage in MPP+ -induced neurodegeneration. *J Neurochem* 115(1):247-258

Chance B, Williams GR, Hollunger G (1963) Inhibition of electron and energy transfer in mitochondria. I. Effects of amytal, thiopental, rotenone, progesterone, and methylene glycol. *J Biol Chem* 238:418–431

Costello J, Castro I, Hacker C, Schrader TA, Metz J, Zeuschner D, Azadi AS, Godinho LF, Costina V, Findeisen P, Manner A, Islinger M, Schrader M (2017) ACBD5 and VAPB mediate membrane associations between peroxisomes and the ER. *J Cell Biol* 216(2):331–342

De Vos KJ, Grierson AJ, Ackerley S, Miller CC (2008) Role of axonal transport in neurodegenerative diseases. *Annu Rev Neurosci* 31:151–73

Dixit E, Boulant S, Zhang Y, Lee AS, Odendall C, Shum B, Hacohen N, Chen ZJ, Whelan SP, Fransen M, Nibert ML, Superti-Furga G, Kagan JC (2010) Peroxisomes are signalling platforms for antiviral innate immunity. *Cell* 141(4):668–681

Fernandez-Gomez FJ, Pastor MD, Garcia-Martinez EM, Melero-Fernandez de Mera R, Gou-Fabregas M, Gomez-Lazaro M, Calvo S, Soler RM, Galindo MF, Jordan J (2006). Pyruvate protects cerebellar granular cells from 6-hydroxydopamine-induced cytotoxicity by activating the Akt signaling pathway and increasing glutathione peroxidase expression. *Neurobiol Dis* 24:296–307

Fransen M, Nordgren M, Wang B, Apanasets O, Van Veldhoven PP (2013) Aging, age-related diseases and peroxisomes. *Subcell Biochem* 69:45–65

Galindo MF, Jordan J, Gonzalez-Garcia C, Cena V (2003) Chromaffin cell death induced by 6-hydroxydopamine is independent of mitochondrial swelling and caspase activation. *J Neurochem* 84:1066–1073

Gao Q, Goodman JM (2015) The lipid droplet—a well-connected organelle. *Front Cell Dev Biol* 3:49

Gomez-Lazaro M, Bonekamp NA, Galindo MF, Jordan J, Schrader M (2008) 6-OHDA induces Drp1-dependent mitochondrial fragmentation in SH-SY5Y cells. *Free Radic Biol Med* 44(11):1960–1969

- Grant P, Ahlemeyer B, Karnati S, Berg T, Stelzig I, Nenicu A, Kuchelmeister K, Crane DI, Baumgart-Vogt E (2013) The biogenesis protein PEX14 is an optimal marker for the identification and localization of peroxisomes in different cell types, tissues, and species in morphological studies. *Histochem Cell Biol* 140(4):423-442
- Higgins DS, Greenamyre JT (1996) [³H]dihydrorotenone binding to NADH: ubiquinone reductase (complex I) of the electron transport chain: an autoradiographic study. *J Neurosci* 16:3807–3816
- Ivashchenko O, Van Veldhoven PP, Brees C, Ho YS, Terlecky SR, Fransen M (2011) Intraperoxisomal redox balance in mammalian cells: oxidative stress and interorganellar cross-talk. *Mol Biol Cell* 22:1440–1451
- Jiang Q, Yan Z, Feng J (2006) Neurotrophic factors stabilize microtubules and protect against rotenone toxicity on dopaminergic neurons. *J Biol Chem* 281:29391–29400
- Koch A, Schneider G, Luers GH, Schrader M (2004) Peroxisome elongation and constriction but not fission can occur independently of dynamin-like protein 1. *J Cell Sci* 117:3995-4006
- Koepke JI, Wood CS, Terlecky LJ, Walton PA, Terlecky SR (2008) Progeric effects of catalase inactivation in human cells. *Toxicol Appl Pharmacol* 232:99–108
- Lin C, Schuster M, Guimaraes SC, Ashwin P, Schrader M, Metz J, Hacker C, Gurr SJ, Steinberg G (2016) Active diffusion and microtubule-based transport oppose myosin forces to position organelles in cells. *Nat Commun* 7:11814
- Lismont C, Nordgren M, Van Veldhoven PP, Fransen M. (2015) Redox interplay between mitochondria and peroxisomes. *Front Cell Dev Biol* 3:35
- Marshall LE, Himes RH (1978) Rotenone inhibition of tubulin self-assembly. *Biochim Biophys Acta* 543:590–594
- Meisner HM, Sorensen L (1966) Metaphase arrest of Chinese hamster cells with rotenone. *Exp Cell Res* 42:291–295

Meurers BH, Zhu C, Fernagut PO, Richter F, Hsia YC, Fleming SM, Oh M, Elashoff D, Dicarolo CD, Seaman RL, Chesselet MF (2009) Low dose rotenone treatment causes selective transcriptional activation of cell death related pathways in dopaminergic neurons in vivo. *Neurobiol Dis* 33(2):182-192

Mohanty A, McBride HM (2013) Emerging roles of mitochondria in the evolution, biogenesis, and function of peroxisomes. *Front Physiol* 4:268

Mounsey RB, Teismann P (2010) Mitochondrial dysfunction in Parkinson's disease: pathogenesis and neuroprotection. *Parkinsons Dis* 2011:617472

Nguyen T, Bjorkman J, Paton BC, Crane DI (2006) Failure of microtubule-mediated peroxisome division and trafficking in disorders with reduced peroxisome abundance. *J Cell Sci* 119(Pt 4):636-45

Nordgren M, Fransen M (2014) Peroxisomal metabolism and oxidative stress. *Biochimie* 98:56–62

Odendall C, Dixit E, Stavru F, Bierne H, Franz KM, Durbin AF, Boulant S, Gehrke L, Cossart P, Kagan JC (2014) Diverse intracellular pathogens activate type III interferon expression from peroxisomes. *Nat Immunol* 15(8):717-726

Peeters A, Fraisl P, van den Berg S, Ver Loren van Themaat E, Van Kampen A, Rider MH, Takemori H, van Dijk KW, Van Veldhoven PP, Carmeliet P, Baes M (2011) Carbohydrate metabolism is perturbed in peroxisome-deficient hepatocytes due to mitochondrial dysfunction, AMP-activated protein kinase (AMPK) activation, and peroxisome proliferator-activated receptor γ coactivator 1 α (PGC-1 α) suppression. *J Biol Chem* 286(49):42162-42179

Peeters A, Shinde AB, Dirkx R, Smet J, De Bock K, Espeel M, Vanhorebeek I, Vanlander A, Van Coster R, Carmeliet P, Fransen M, Van Veldhoven PP, Baes M (2015) Mitochondria in peroxisome-deficient hepatocytes exhibit impaired respiration, depleted DNA, and PGC-1 α independent proliferation. *Biochim Biophys Acta* 1853(2):285-298

- Perez-Ortiz JM, Tranque P, Vaquero CF, Domingo B, Molina F, Calvo S, Jordan J, Cena V, Llopis J (2004) Glitazones differentially regulate primary astrocyte and glioma cell survival. Involvement of reactive oxygen species and peroxisome proliferator-activated receptor-gamma. *J Biol Chem* 279:8976-8985
- Piperno G, LeDizet M, Chang XJ (1987) Microtubules containing acetylated alpha-tubulin in mammalian cells in culture. *J Cell Biol* 104(2):289-302
- Ren Y, Liu W, Jiang H, Jiang Q, Feng J (2005) Selective vulnerability of dopaminergic neurons to microtubule depolymerization. *J Biol Chem* 280(40):34105-12
- Ribeiro D, Castro I, Fahimi HD, Schrader M (2012) Peroxisome morphology in pathology. *Histol Histopathol* 27(6):661-76
- Schrader M, Baumgart E, Fahimi HD (1995) Effects of fixation on the preservation of peroxisomal structures for immunofluorescence studies using HepG2 cells as a model system. *Histochem J* 27:615-619
- Schrader M, Bonekamp N, Islinger M (2012) Fission and proliferation of peroxisomes. *Biochim Biophys Acta – Molecular Basis of Disease* 1822(9):1343-1357
- Schrader M, Burkhardt JK, Baumgart E, Lüers G, Spring H, Völkl A, Fahimi HD (1996) Interaction of microtubules with peroxisomes. Tubular and spherical peroxisomes in HepG2 cells and their alterations induced by microtubule-active drugs. *Eur J Cell Biol* 69:24-35
- Schrader M, Costello J, Godinho LF, Azadi AS, Islinger M (2016) Proliferation and fission of peroxisomes – an update. *Biochim Biophys Acta – Molecular Cell Research* 1863:971-983
- Schrader M, Costello J, Godinho LF, Islinger M (2015a) Peroxisome-Mitochondria Interplay and Disease. *J Inherit Metab Dis* 38(4):681-702
- Schrader M, Fahimi HD (2006) Growth and Division of Peroxisomes. *Int Rev Cytology* 255:237-290
- Schrader M, Godinho LF, Costello J, Islinger M (2015b) The different facets of organelle interplay—an overview of organelle interactions. *Front Cell Dev Biol* 3:56

- Schrader M, Grille S, Fahimi HD, Islinger M (2013) Peroxisome interactions and cross-talk with other subcellular compartments in animal cells. *Subcell Biochem* 69:1-22
- Schrader M, Krieglstein K, Fahimi HD (1998) Tubular peroxisomes in HepG2 cells: Selective induction by growth factors and arachidonic acid. *Eur J Cell Biol* 75:87-96
- Schrader M, Thiemann M, Fahimi HD (2003) Peroxisomal Motility and Interaction with Microtubules. *Micr Res Tech* 61:171-178
- Schrader M, Wodopia R, Fahimi HD (1999) Induction of tubular peroxisomes by UV irradiation and reactive oxygen species in HepG2 cells. *J Histochem Cytochem* 47:1141-1148
- Schrader M, Yoon Y (2007) Mitochondria and peroxisomes: Are the "big brother" and the "little sister" closer than assumed? *BioEssays* 29(11):1105-1114
- Sherer TB, Betarbet R, Testa CM, Seo BB, Richardson JR, Kim JH, Miller GW, Yagi T, Matsuno-Yagi A & Greenamyre JT (2003) Mechanism of toxicity in rotenone models of Parkinson's disease. *J Neurosci* 23:10756–10764
- Srivastava P, Panda D (2007) Rotenone inhibits mammalian cell proliferation by inhibiting microtubule assembly through tubulin binding. *FEBS Journal* 274:4788–4801
- Sugiura A, Mattie S, Prudent J, McBride HM (2017) Newly born peroxisomes are a hybrid of mitochondrial and ER-derived pre-peroxisomes. *Nature* 542(7640):251-254
- Testa CM, Sherer TB, Greenamyre JT (2005) Rotenone induces oxidative stress and dopaminergic neuron damage in organotypic substantia nigra cultures. *Mol Brain Res* 134:109
- Titorenko VI, Terlecky SR (2011) Peroxisome metabolism and cellular aging. *Traffic* 12(3):252-259.
- Walton PA, Pizzitelli M (2012) Effects of peroxisomal catalase inhibition on mitochondrial function. *Front Physiol* 3:108
- Wanders RJ, Waterham HR (2006) Peroxisomal disorders: the single peroxisomal enzyme deficiencies. *Biochim Biophys Acta* 1763:1707–1720

Wanders RJ, Waterham HR, Ferdinandusse S (2016) Metabolic Interplay between Peroxisomes and Other Subcellular Organelles Including Mitochondria and the Endoplasmic Reticulum. *Front Cell Dev Biol* 3:83

Wang B, Van Veldhoven PP, Brees C, Rubio N, Nordgren M, Apanasets O, Kunze M, Baes M, Agostinis P, Fransen M (2013) Mitochondria are targets for peroxisome-derived oxidative stress in cultured mammalian cells. *Free Radic Biol Med* 65:882-894

Wiemer EA, Wenzel T, Deerinck TJ, Ellisman MH, Subramani S (1997) Visualization of the peroxisomal compartment in living mammalian cells: dynamic behavior and association with microtubules. *J Cell Biol* 136(1):71-80

Figure legends

Fig. 1 Rotenone induces alterations in peroxisome morphology and distribution. COS-7 cells were treated with solvent (CON) or rotenone (ROT) for 6 and 24 hours and processed for immunofluorescence microscopy using antibodies directed to PEX14, a peroxisomal membrane protein. **(a-d)** Representative examples. **(a)** Control (CON). Note the elongated tubular peroxisomes in **(b)** (1 mM ROT, 6 hours), the formation of peroxisomal clusters **(c)**, arrowheads) (100 μ M ROT, 6 hours), and the non-uniform distribution of peroxisomes **(d)** (100 μ M ROT, 6 hours) in contrast to **(a)**. Boxed region in **(b)** shows higher magnification view. **(e, f)** Qualitative assessment of peroxisome elongation **(e)** and cluster formation **(f)**. A minimum of 150 cells were examined per condition, and organelle morphology and distribution was microscopically assessed. Values represent mean \pm SD of at least 3 independent experiments. N, nucleus. Bar, 10 μ m.

Fig. 2 Rotenone induces microtubule depolymerisation and acetylation of α -tubulin in COS-7 cells. **(a-f)** Cells were treated with solvent **(a)** (CON) or different concentrations of rotenone (ROT) **(b-f)** for 6 hours and processed for immunofluorescence microscopy using antibodies directed to α -tubulin. **(g-i)** Cells were treated with solvent **(g)** (CON), 100 nM rotenone **(h)** or 1 μ M rotenone **(i)** for 3 hours and labelled with antibodies directed to acetylated α -tubulin. **(j)** Immunoblot of cell lysates showing levels of acetylated α -tubulin after 3 hours of rotenone treatment. 50 μ g of protein were loaded and the blot probed with acetylated α -tubulin and α -tubulin antibody as indicated. α -tubulin serves as loading control. Bars, 10 μ m.

Fig. 3 Microtubule stabilisation prevents rotenone-induced clustering of peroxisomes. COS-7 cells were treated with solvent (CON) **(a, e)**, paclitaxel (TAX) **(b, f)**, paclitaxel and 100 μ M rotenone (ROT) **(c, g)**, or paclitaxel and 1 mM rotenone **(d, h)** for 6 and 24 hours. Cells were then processed for immunofluorescence microscopy using antibodies directed to α -tubulin **(a-**

d) or PEX14 (**e-h**). **(i)** Qualitative assessment of peroxisome cluster formation. A minimum of 150 cells were examined per condition, and organelle distribution was microscopically assessed. Values represent mean \pm SD of at least 3 independent experiments. P-values refer to appropriate controls unless indicated. Bar, 10 μ m.

Fig. 4 Antioxidant treatment reduces rotenone-induced intracellular ROS levels, but does not prevent peroxisomal clustering. **(a)** Determination of intracellular ROS levels using the fluorescent dye 2', 7'-dichlorodihydrofluorescein diacetate (H₂DCFDA) after treatment of COS-7 cells with the antioxidant N-acetyl cysteine (NAC), 100 nM rotenone (ROT), or N-acetyl cysteine and 100 nM rotenone. Data are expressed as percentage of control (mean \pm SD) and are from 3 independent experiments. **(b)** Qualitative assessment of peroxisome cluster formation (as described for Fig. 3). Cells were treated as indicated and processed for immunofluorescence microscopy using antibodies directed to PEX14. Values represent mean \pm SEM of at least 3 independent experiments. P-values refer to appropriate controls unless indicated.

Fig. 5 Rotenone-induced mitochondrial fragmentation can be prevented by antioxidant-treatment but not by microtubule stabilization. **(a-d)** Rotenone induces the formation of spherical mitochondria. COS-7 cells were treated with solvent (CON) **(a)** or rotenone (ROT) for 6 **(b, c, d)** and 24 hours **(d)** and processed for immunofluorescence microscopy using antibodies directed to TOM20, a mitochondrial outer membrane protein. Note the elongated tubular mitochondria in **(a)** in contrast to **(b, c)**. **(d)** Qualitative assessment of mitochondrial morphology. A minimum of 150 cells were examined per condition, and organelle morphology was microscopically assessed. Values represent mean \pm SD of at least 3 independent experiments. **(e-h)** Microtubule stabilisation does not prevent rotenone-induced mitochondrial fragmentation. COS-7 cells were treated with paclitaxel (TAX) **(e)** or paclitaxel

and rotenone (ROT) for 6 (**f**, **g**, **h**) and 24 hours (**h**) and labelled with TOM20 antibodies. Note the elongated tubular mitochondria in (**e**) in contrast to (**f**, **g**). (**h**) Qualitative assessment of mitochondrial morphology (see above). (**i-l**) Antioxidant-treatment prevents rotenone-induced mitochondrial fragmentation. COS-7 cells were treated with N-acetyl cysteine (NAC) (**i**) or N-acetyl cysteine and rotenone (ROT) for 3 (**j**, **k**, **l**) and 6 hours (**l**) and labelled with TOM20 antibodies. Note the elongated tubular mitochondria in (**j**, **k**, **l**) in contrast to (**b**, **c**, **f**, **g**). (**l**) Qualitative assessment of mitochondrial morphology (see above). P-values refer to appropriate controls unless indicated. Bars, 10 μm .

Fig. 1

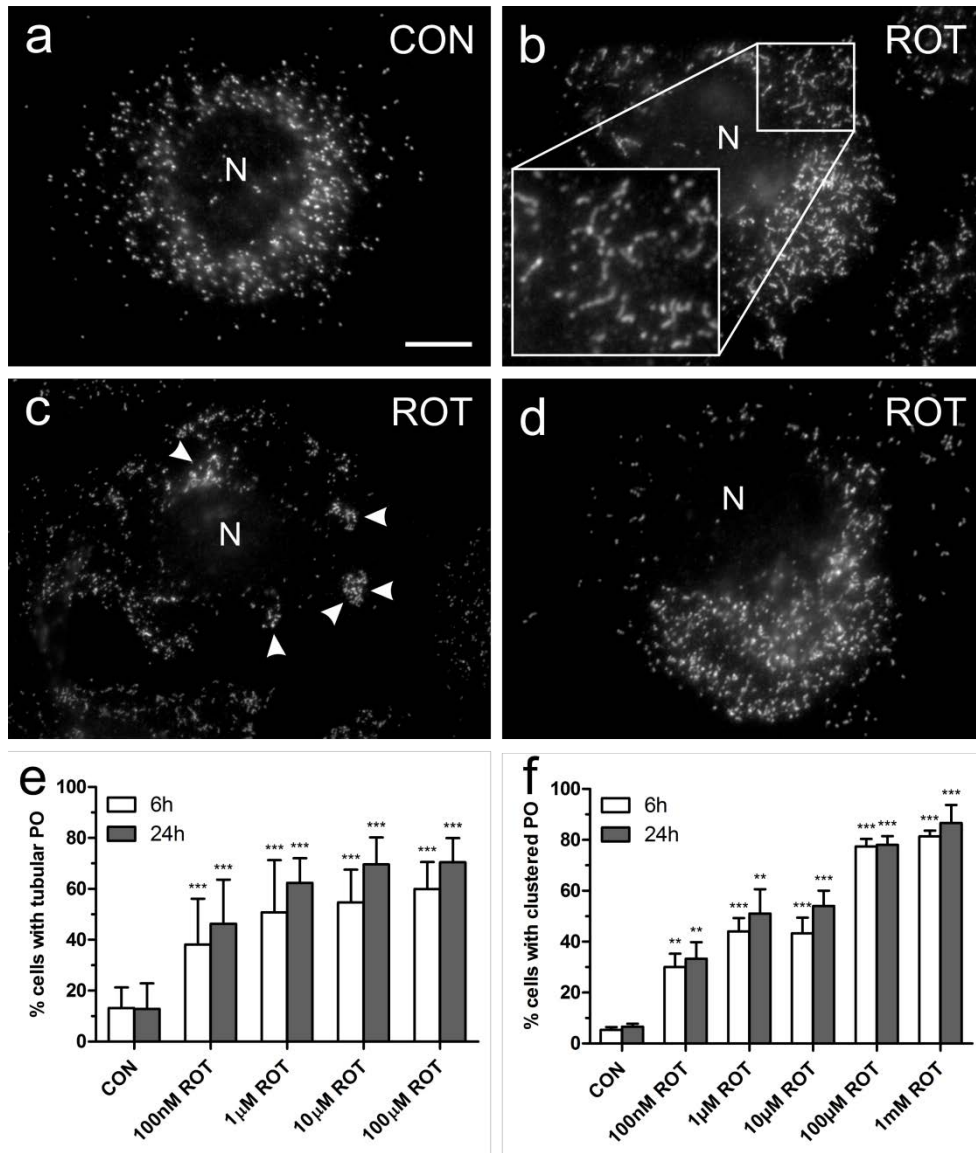


Fig. 2

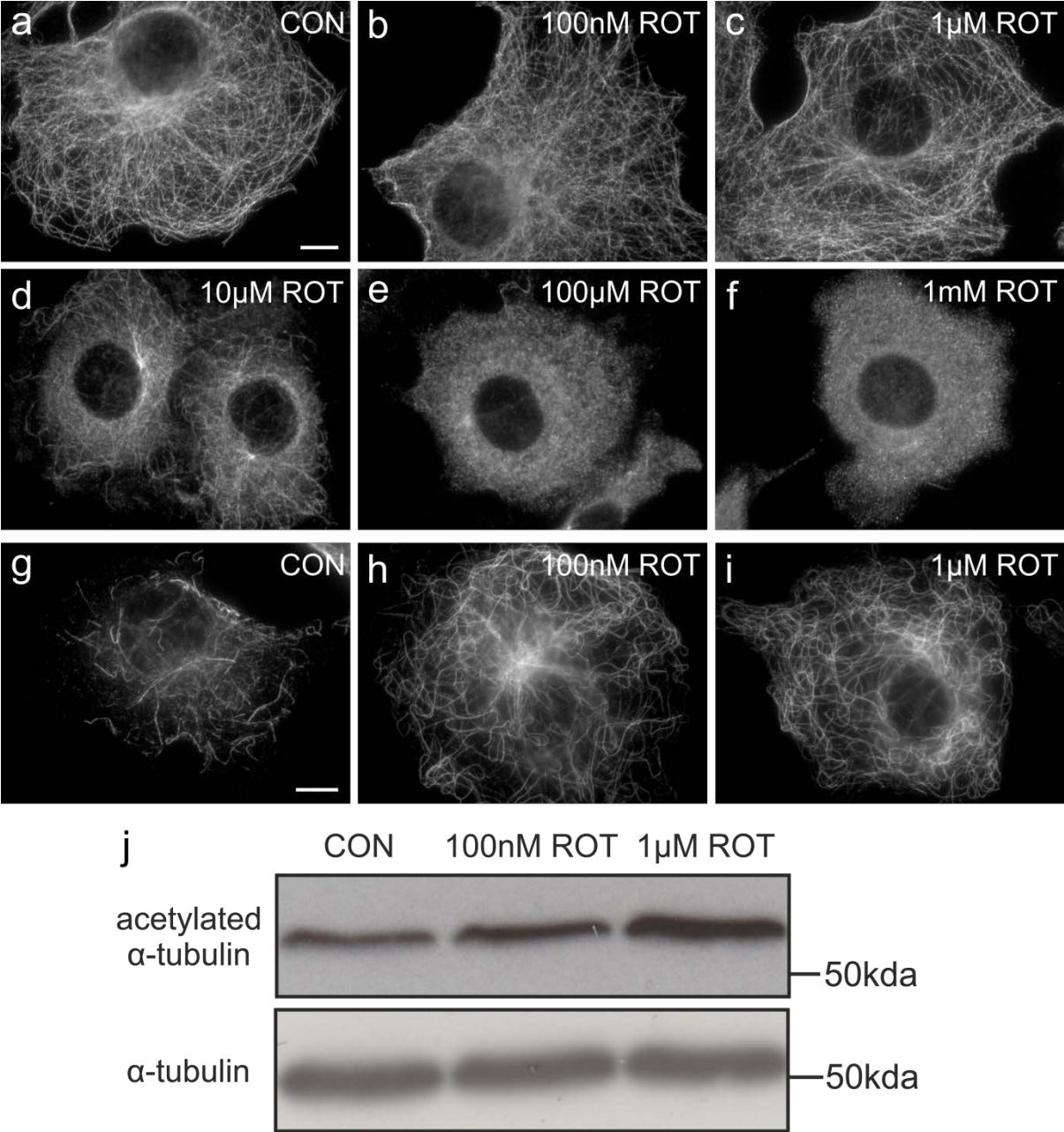


Fig. 3

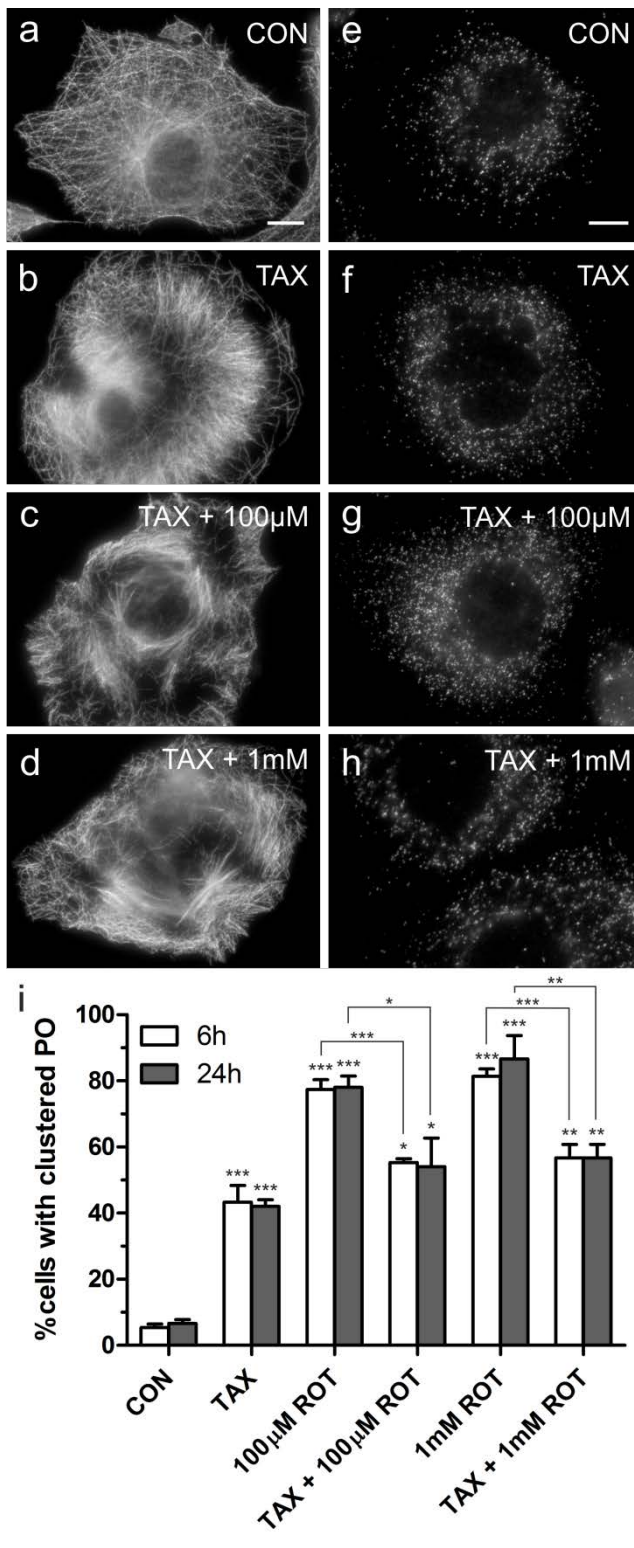


Fig. 4

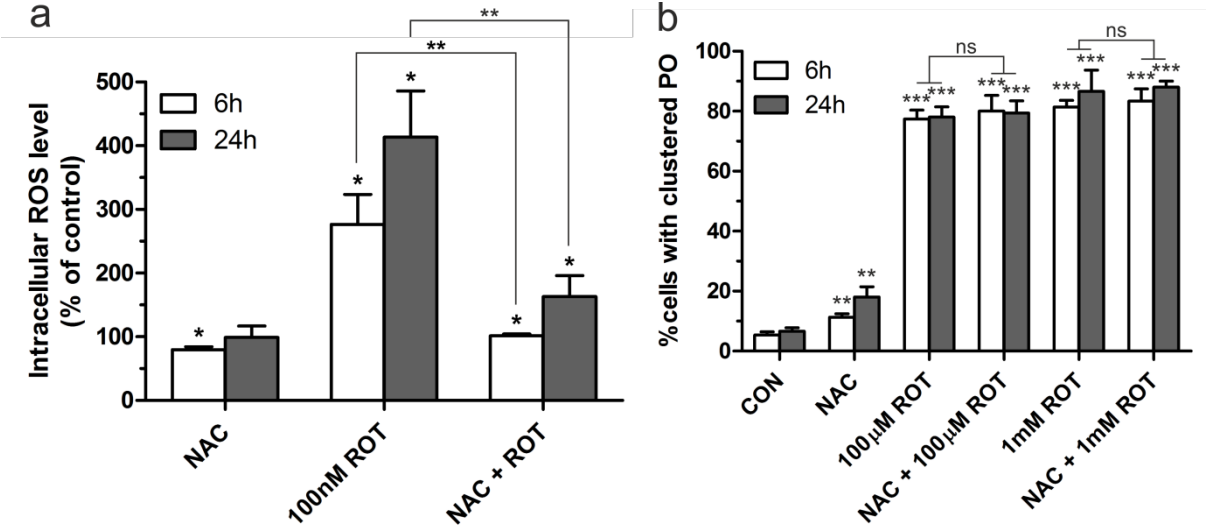


Fig. 5

